since 1961

Baltica

BALTICA Volume 34 Number 1 June 2021: 58–70
https://doi.org/10.5200/baltica.2021.1.5

A comprehensive spatiotemporal evaluation of the current earthquake activity in different parts of the Frakull-Durrës fault zone, Albania

Serkan Öztürk*, Rrapo Ormeni

Öztürk, S., Ormeni, R. A comprehensive spatiotemporal evaluation of the current earthquake activity in different parts of the Frakull-Durrës fault zone, Albania. *Baltica, 34 (1)*, 58–70. Vilnius. ISSN 0067-3064.
Manuscript submitted 16 December 2020 / Accepted 12 April 2021 / Available online 20 June 2021

Abstract. This study presents a detailed spatiotemporal analysis for the Frakull-Durrës (F-D) fault zone at the beginning of 2020. For this purpose, the most frequently used statistical seismicity parameters such as magnitude completeness, *Mc*-value, Gutenberg-Richter *b*-value, recurrence times, annual probabilities and standard normal deviate, Z-value, were mapped. The F-D fault zone was divided into two seismogenic subregions, and *Mc*-value was taken as 2.5 for both the south and north parts. The *b*-value was estimated as 0.83 ± 0.06 for the south part and 0.85 ± 0.06 for the north part. *b*-values for both zones are smaller than 1.0 and these values may be considered to be a larger stress accumulation to build up over time and to be released by the next possible earthquakes. Clear decreasing trends were observed in time variations of *b*-values before the occurrences of several strong main shocks. Analyses of annual probabilities and recurrence times suggest that the study region has an intermediate/long-term earthquake hazard in comparison to occurrences of strong/destructive earthquakes in the short term. Some anomaly regions of a small *b*-value and a large Z-value were found along the F-D fault zone at the beginning of 2020: *i*) among Lushnje-Tirana-Durrës including the middle part of the F-D fault zone, *ii*) in and around Lezha including the north end of the F-D fault zone. Thus, the combination of regions with the lowest *b*-value and largest *Z*-value may supply preliminary results for earthquake hazard, and these regions may be considered to be the most likely regions for future strong/large earthquakes in the F-D fault zone.

Keywords: *seismicity; b-value; Z-value; recurrence time; annual probability; earthquake hazard*

Serkan Öztürk (serkanozturk@gumushane.edu.tr), Gümüşhane University, Department of Geophysics, 29100, Gümüşhane, Turkey; Rrapo Ormeni (rrapo55@yahoo.com) Institute of Geosciences, Energy, Water and Environment, Polytechnic University of Tirana, Don Bosko Str. 60, Albania*
**Corresponding author at Gümüşhane University, Department of Geophysics, TR-29100, Gümüşhane, Turkey. Email: serkanozturk@gumushane.edu.tr*

INTRODUCTION

The Albania region is one of the most seismically active regions with tens of large destructive earthquakes since the earliest recorded history and from the historical sources (Sulstarova *et al*. 1980; Aliaj *et al*. 2010). The Frakull-Durrës (F-D) fault zone in Albania has been a seismically active area from the historical sources and currently with high seismicity. The main reason for seismicity in Albanian is the collision of the Adria microplate with the Albanian orogen. The Adriatic microplate has played a major role in the tectonic history of the central Mediterranean region. This continental collision directly influences the external part of the country, the longitudinal faults cutting across the western part of Albania (Aliaj *et al*. 2001; Ormeni *et al*. 2013).

The F-D fault zone is located in the front of collision of the Adriatic microplate with the Albanian orogen. The F-D fault zone is placed in the west of the external area, between the Lezha-Ulqini fault and the Vlora-Tepelena transverse flexure. Seismic data and focal mechanism solutions show that this fault zone is associated with thrusts or back-thrusts. Compressional deformation in the F-D fault zone is present nowadays. The F-D fault zone is the main part of the Ioniano-Adriatic longitudinal fault zone in Albania and is a major tectonic feature with a well-defined fault trace and an established history of seismicity. Old chronological results show that this town was almost totally destroyed in the years 177 B.C, 334 or 345 A.D., 506, 1273, 1279, 1869 and 1870. Earthquake activity of the F-D fault zone during the 20th century began with a series of destructive Durrës earthquake *M*6.2 in 1926 and Fieri earthquake *M*6.0 in 1962 (Sulstarova *et al*. 1980; Aliaj *et al*. 2001). Currently, the seismicity of Durrës region is characterized by a series of the high-energy/strong earthquakes on 21 September, $M_L = 5.8$ which was followed two months later by another, strongest shock of 26 November 2019, of the magnitude $M_L = 6.3$ (Ormeni *et al*. 2020).

There are a lot of region-time-magnitude studies on the characteristics of earthquake activity for different parts of the world, and many authors obtained very important outcomes by using scaling laws (e.g., Frohlich, Davis 1993; Wiemer, Wyss 2000; Öncel, Wilson 2002; Polat *et al*. 2008; Öztürk 2013, 2017, 2020; Ali 2016; Rodriguez-Perez, Zuniga 2018; Radziminovich *et al*. 2019; Zuniga *et al*. 2020). In the scope of this study, we made a detailed spatiotemporal analysis of the earthquakes along the F-D longitudinal fault zone in order to evaluate the seismic hazard potential at the beginning of 2020. From this point of view, this work is focused on the imaging of size-scaling distributions such as regional, temporal and magnitude distribution of earthquake activity, magnitude completeness, *Mc*, seismotectonic *b*-value and its variations with time, precursory seismic quiescence *Z*-value, annual probability and recurrence time. *ZMAP* analysis software (Wiemer 2001) was used for all statistical estimations and for all histograms of regional, temporal and magnitude distribution along the F-D fault zone.

Neotectonic structures of Albania

Albania is situated in the Alpine-Mediterranean seismic belt and accommodates part of the deformation due to the collision of the Adriatic microplate with the Eurasian plate (Mazzoli, Helman 1994). Geographically, it is surrounded by Montenegro and Kosovo in the north, the former Yugoslav Republic of Macedonia (FYROM) in the east, Greece in the south and southeast, and the Adriatic and Ionian Seas in the west. The Adriatic collision zone is the most seismically active region in Albania and makes up the Ionian-Adriatic coastal earthquake belt at the eastern margin of the Adria microplate. The present-day tectonic stress field has been well studied via microtectonics (Aliaj 2012) and focal mechanism solutions of earthquakes (Sulstarova 1986; Muço 1994, 2007; Aliaj *et al*. 2010; Ormeni *et al*. 2013; Aliaj, Meço 2018). In the external domain, the average axis of compression is in the NE-SW direction (average azimuth 225°). Four large neotectonic units have been recognised based on the tectonic regime and the type of deformation (Aliaj *et al*. 2010) as follows (Fig. 1):

i) The Internal unit affected by post-Pliocene-Quaternary extensional tectonics;

ii) The External unit affected by pre-Pliocene (since the end of Oligocene and the middle Miocene) compressional regime, continuing to be active up to the present time;

iii) The Peri-Adriatic Depression affected by post-Pliocene (since the Pliocene until the present) compressional regime;

iv) The Foreland in Adriatic and Ionian offshore, non-deformed or weakly deformed by normal faulting.

The Albanian orogenic thrust front is cut and displaced by the Othoni Island-Dhermi, the north Sazani Island and the Gjiri i Drinit-Lezha strike-slip faults, which divide the orogeny into separate segments with diachronous development (Fig. 1; Aliaj 2006):

i) The NW-trending Lefkas-Corfou offshore segment, where the Ionian zone consists of the orogenic front;

ii) The NW-trending Karaburuni-Sazani Island offshore segment, where the Sazani zone comprises the orogenic front;

iii) The N-trending Frakull-Durrës mainly onshore segment, where Ionian zone makes up this orogenic front;

iv) The WNW-trending Lezha-Ulqini segment, where the orogenic front is composed of the Kruja zone.

The ~N-trending Frakull-Durrës (mainly onshore) anticline segment

In the north of an E-W-trending transverse fault near Sazani Island, the transition from the Apulian platform to the Albanian Basin (South Adriatic Basin) occurs in the Adriatic offshore (Fig. 1). The front of the orogen is buried under molasses of Middle Miocene age exposed onshore on coastal terrains of the Periadriatic depression and may pass along the Frakull-Durrës anticlinal segment of quasi-northern extension (Bega 1995; Kociu 1998). Earthquake activity shows that the Mio-Pliocene anticlines of Periadriatic depression are associated with a thrust or back-thrust faults (Biçoku 1964). These terms are called over-fault anticlines or determined by Biçoku (1964) as having been “placed in narrow zones of some big faults found under the Neogene cover”. The north-trending Frakull-Durrës anticline (Fig. 1) has been subjected to dextral transpressional deformation associated with the oblique northeast-southwest regional horizontal compression in post-Pliocene time. In the Durrës anticline, the main fault is a west-dipping back-thrust that cuts marine Quaternary sediments that are still horizontal. The orogenic front along the Frakull-Durrës segment is marked at the surface by thrusting and back-thrusting. Along the Ardenica and Durrës anticlines, the Oligocene to Quaternary age thick clastic sediments of South Adriatic Basin (Albanian Basin) have been detached from their carbonate substratum and have glided along a decollement at the level of the Oligocene clastics (Aliaj 2006).

Earthquake database and subregions for the F-D fault zone

As stated above, during the historical and instrumental periods, many strong/destructive earthquakes occurred in the F-D fault zone (Fig. 2a). The F-D fault

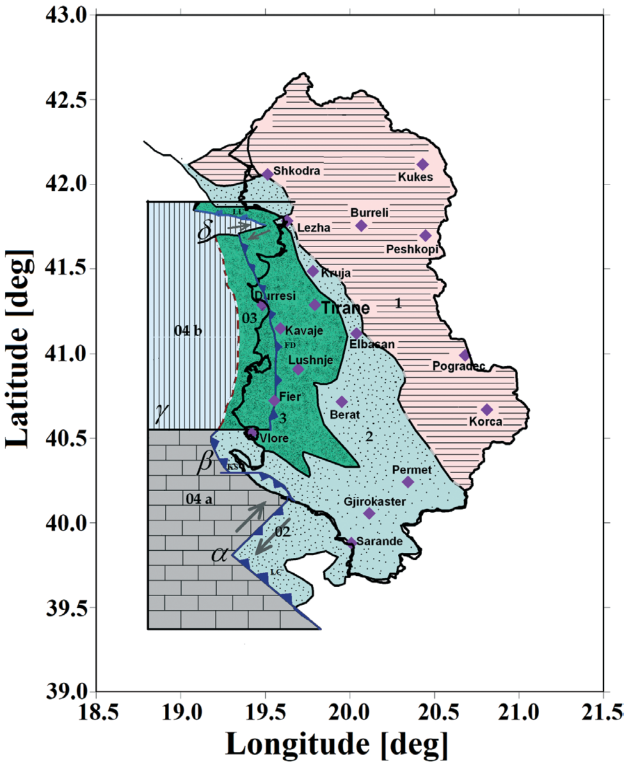

Fig. 1 Map of neotectonic (Pliocene-Quaternary) zonation of Albania (from Aliaj 2000, modified from Ormeni *et al.* 2020). Four large neotectonic units are noted by numbers on the map: 1. Internal unit; 2. External unit (02 = its offshore sectors); 3. Periadriatic Foredeep (03 = its offshore sector); 4. Foreland in offshore (04a = Apulian platform, 04b = Albanian Basin). The Albanian orogenic front is cut and displaced by, from south to north, the Othoni Island-Dhermi (α), the Gjiri i Ariut-Dukat (β), the north Sazani Island (γ), and the Gjiri i Drinit-Lezha (δ) strike-slip faults. Respectively, frontal thrusts are LC: Lefkas-Corfu, KS: Karaburuni-Sazani Island, F-D: Frakull-Durrës, and LU: Lezha-Ulqini

has generated many destructive earthquakes from the historical period of time 58 to the instrumental period of 2019 such as 4 February 1934 (*M*5.6), 18 March 1962 (*M*6.0) and 19 August 1970 (*M*5.5), 21 September 2019 (*M*5.8) and 26 November 2019 (*M*6.3). The Durrës section has ruptured during the earthquakes occurred on 17 December 1926 (*M*6.2).

The earthquake database used in this study contains a total of 2310 events occurred along the F-D fault zone. Magnitude type used for the statistical analyses is local magnitude, M_L. Earthquake catalog is complete for all magnitude sizes and for all time intervals between 1967 and 2020. Earthquake epicentres with $1.0 \leq M_L \leq 6.3$ and strong main shocks with $M_L \geq 5.0$ are shown in Fig. 2b. Also, a figure for the earthquake distributions with different magnitude levels in and around the F-D fault zone was shown with different symbols in the same figure. Some details for the earthquakes with magnitude $M_L \geq 5.0$ are given in Table 1. The depth of earthquakes considered in this study was limited to shallow earthquakes less than 90 km because these types of earthquake statistical analyses for future seismic hazard, especially in detecting the precursory seismic quiescence, have provided important results related to the crustal main shocks. In addition to this general approach, the analyses of focal depths reveal that the seismicity in the study region was mainly generated in the middle and lower crust (Ormeni 2007, 2010).

As shown in Fig. 2b, the study region was divided into two parts: the south part (region 1) and the north part (region 2) of the F-D fault zone. The original catalog includes 2310 earthquakes between 20 July 1967 and 31 December 2019, and time period is about 52.45 years. After the selection of different parts of the study region, earthquake databases in these areas were prepared for the analyses. The final data catalogs include 708 earthquakes for region 1, and 1602 earthquakes for region 2, with $M_L \geq 1.1$ and depth < 90 km.

METHODOLOGY AND STATISTICAL PARAMETERS

In this study, spatiotemporal analyses of earthquake distribution were limited to shallow earthquakes with depths less than 90 km. The maximum depth was selected as 90 km because it is generally assumed that the seismogenic layer is about this depth for different parts of the world. As mentioned above, focal mechanism solutions in the study area show that seismic activity is mainly produced in the middle and lower crust due to tectonic situations (Ormeni *et al.* 2020). Also, some statistical analyses including the studies of precursory seismic quiescence supply important results for the crustal main shocks in reveal-

Table 1 Detailed information of earthquakes occurred in the F-D fault zone with magnitude $5.0 \leq M_L \leq 6.3$ from 1967 to 2020

Date	Origin Time	Latitude	Longitude	Depth (km)	M_L	Subregion	Place	Epicentral Intensity (Io)
16/11/1982	23:41:21.00	40.77	19.58	13	5.7	1	Rroskovec	VII–VIII
09/01/1988	01:02:46.00	41.22	19.81	5	5.3	1	Tirana	VII
12/05/1997	13:51:34.00	41.19	19.63	40	5.0	1	Kavaj	VI
26/09/1997	09:41:35.00	41.31	19.18	76	5.5	2	Adriatic Sea	VI
12/04/1998	11:57:05.00	41.22	19.39	20	5.8	1	Adriatic Sea	VII–VIII
04/07/2018	09:00:45.00	41.47	19.51	18	5.1	2	Durrës	VI–VII
02/09/2019	14:04:23.00	41.42	19.51	29	5.8	2	Durrës	VII–VIII
21/09/2019	14:15:52.00	41.45	19.47	38	5.3	2	Durrës	VI–VII
26/11/2019	02:54:11.00	41.46	19.44	39	6.3	2	Adriatic Sea	VIII–IX
26/11/2019	06:08:23.00	41.62	19.51	34	5.5	2	Kepi Rodonit	VII
27/11/2019	14:45:24.00	41.67	19.38	48	5.3	2	Adriatic Sea	VI–VII
28/11/2019	10:52:43.00	41.56	19.58	25	5.0	2	Lalez	VI

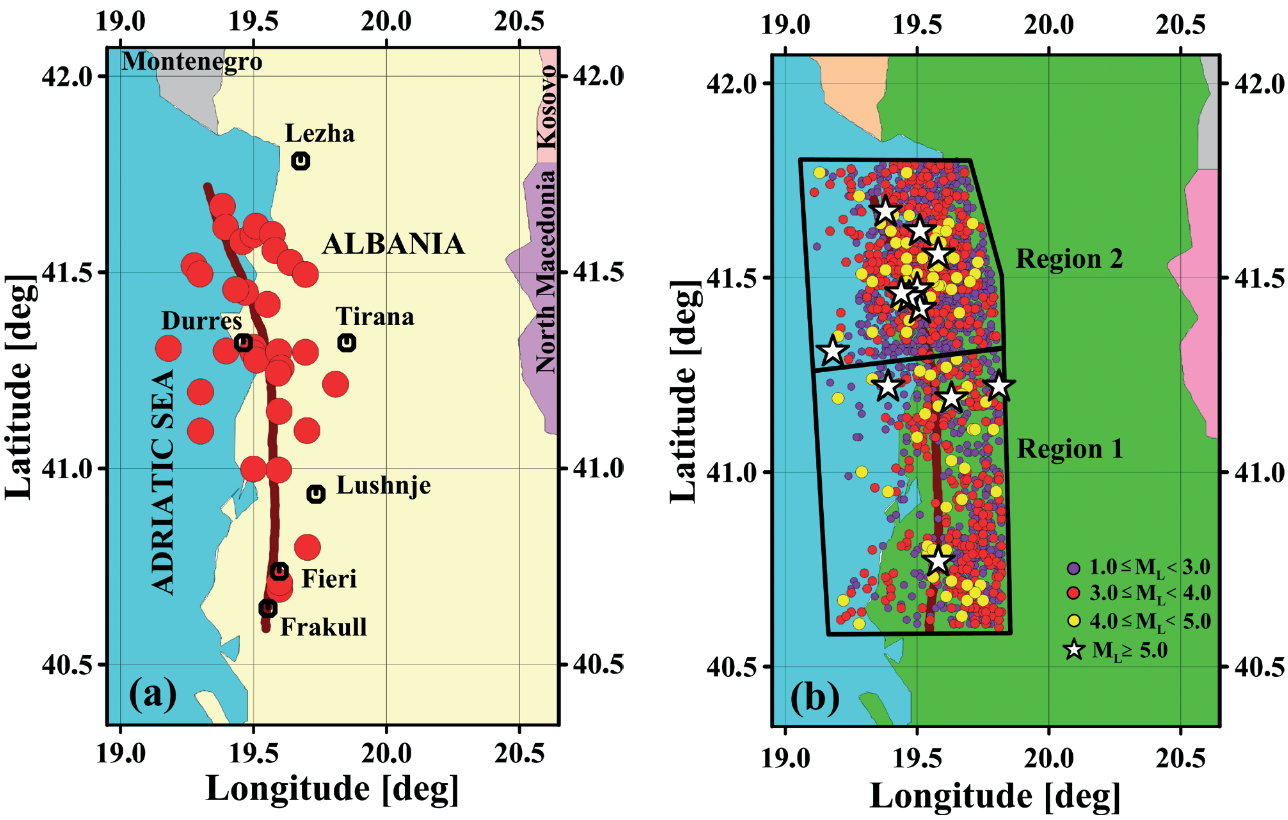

Fig. 2(a) Epicentre distributions of earthquakes with $M_L \geq 5.0$ in and around the F-D fault zone during the period of time 58–2019. **(b)** Epicentre distributions of all events with $M_L \geq 1.1$ in the F-D fault zone between 1967 and 2020. Subregions are also plotted on the figure

ing the possible seismic hazard. To describe the behaviours of earthquake activity in the F-D fault zone, the best known statistical parameters were evaluated: time-magnitude histograms of earthquake distribution, spatiotemporal distributions of seismotectonic *b*-value, precursory seismic quiescence *Z*-value, annual probability and recurrence time.

Gutenberg-Richter relation (*b*-value), annual probability, recurrence time and magnitude completeness (*Mc*-value)

The size-scaling distribution of earthquakes is described by Gutenberg and Richter (G-R) relation (Gutenberg, Richter 1944). This relation between the frequency of occurrence and earthquake magnitudes can be given with the following formula:

$$\log_{10} N(M) = a - bM, \quad (1)$$

where *N(M)* is the cumulative number of events with magnitudes larger than or equal to *M* in a given time period, while *a*- and *b*-values are constants. The *a*-value is related to the seismic activity level, and variations in *a*-value depend on the extend of the study area and time interval of the catalog. Therefore, *a*-value shows important variations in different parts of the world in relation to the earthquake activity level. The *b*-value is one of the most significant statistical parameters in terms of the seismotectonic properties in a specific area. The *b*-value can be calculated from the slope of magnitude-frequency distribution. It is suggested generally that the *b*-value varies from 0.3 to 2.0 from region to region in different parts of the world (Utsu 1971). Also, Frohlich, Davis (1993) described the average *b*-value as close to 1.0. Although *b*-value reflects the relative numbers of small and great earthquakes, it is, in fact, a very important parameter in terms of rheological and geotechnical perspective. Many studies suggest that the *b*-value is scale invariant, and it is related to the distribution of earthquake epicenters and fault segments. Many factors affect the changes in *b*-values: an increase in thermal gradient, fracture density, material heterogeneity in the geological complexity, the number of small and large earthquakes, fault length, stress and strain conditions (Mogi 1962). Previous studies suggest that the *b*-value is also related to the fault length, material properties, strain circumstances, stress and slip distribution, *etc*., and it is scale invariant.

Annual probabilities of any earthquakes for different magnitude sizes and for any periods can be calculated from the following equation (Ali 2016; Öztürk 2020):

$$P(M) = 1 - e^{-N(M)*T}, \quad (2)$$

where *P(M)* is the probability that at least one event will occur in specific *T* years. *M* is taken from Equation 1. Also, return periods of any earthquakes for different magnitude levels can be calculated from the following formula (Ali 2016; Öztürk 2020):

$$Q = 1 / N(M). \quad (3)$$

Magnitude completeness, *Mc*-value, is a very important parameter for the statistical seismicity studies. *Mc*-value is the minimum magnitude of complete recording and can be calculated from frequency-magnitude distribution of earthquakes (Wiemer, Wyss 2000). This magnitude level contains the 90% of the events in the catalog, and temporal changes in *Mc*-value can affect the results of the seismicity parameters, especially in *b*- and *Z*-values. Hence, it is aimed to use the maximum number of earthquakes in the catalog for high-quality results of all statistical parameters.

Declustering process and standard normal deviate *Z*-test

Some secondary events such as foreshocks, aftershocks or earthquake swarms frequently mask the spatiotemporal distributions of the earthquakes and thus related earthquake statistics. Therefore, all dependent events should be excluded from the catalog to realize a quantitative seismicity analysis. Arabasz, Hill (1996) explained that cluster analysis process "declusters" or decomposes a catalog into the primary and secondary events. This declustering process eliminates all dependent events from each cluster and all dependent earthquakes are replaced as a single earthquake.

In this study, Reasenberg (1985) algorithm was used to decluster the catalog through *ZMAP* software and region-time distributions of seismotectonic parameters such as *b*-value, *Z*-value and recurrence time calculated by using the resulting declustered data. There are 708 earthquakes with $M_L \geq 1.3$ in region 1 (south part) of the F-D fault zone. The declustering process eliminated 76 events, and 632 earthquakes were obtained. *Mc*-value was computed as 2.5 for this part, and the events with magnitudes smaller than 2.5 were excluded from the declustered catalog. The number of events exceeding this completeness magnitude level is 143. These two processes removed 219 events, and in total, 30.93% of the earthquakes were removed from the catalog of region 1. The earthquake catalog for the statistical analysis includes 489 earthquakes in the south part of the F-D fault zone. There are 1602 events with $M_L \geq 1.1$ in region 2 (north part) of the F-D fault zone. The declustering procedure removed 463 events and resulted in 1139 earthquakes. *Mc*-value was estimated as 2.5 for region 2, and earthquakes with $M_L < 2.5$ are excluded from the declustered catalog. The number of events exceeding this *Mc*-value is 540. These two procedures removed 1003 events, and 62.61% of the events in total are removed from the catalog of region 2. Consequently, the earthquake catalog for statistical assessments consists of 599 events in the north part of the F-D fault zone.

There are many statistical models describing and evaluating the earthquake activity rate changes and many of them use spatiotemporal modelling of seismic quiescence before the main shocks. One of the most used technique for these types of calculations can be given as the standard normal deviate *Z*-test. *ZMAP* algorithm is used to map the regions showing seismic quiescence (for details, see Wiemer, Wyss

1994). Standard normal deviate Z-test generates the Long Term Average, LTA (t) function for the statistical assessment of the confidence level in standard deviation units:

$$Z(t) = (R_1 - R_2) / \left(\frac{\sigma^2{}_1}{n_1} + \frac{\sigma^2{}_2}{n_2} \right)^{1/2}, \tag{4}$$

where R_1 is the average number of earthquakes in the foreground window, R_2 is the average seismic activity rate in the whole background period, σ and n are the standard deviations and the number of samples within and outside the window. The Z-value calculated as a function of time lets the foreground window slide along the duration of the catalog and is named as LTA (t).

RESULTS AND DISCUSSION

In this study, a comprehensive spatiotemporal assessment of the earthquake activity including the F-D fault zone and its surrounding area, Albania, was performed by analyzing the most frequently used seismotectonic parameters such as b-value, Z-value, annual probabilities, recurrence times and also by mapping the region-time-magnitude histograms between 1967 and 2020. With the evaluation of these arguments, we tried to make an estimation and interpretation for the future earthquake potential in and around the F-D fault zone.

Cumulative numbers of the earthquakes as a function of time for the south (region 1) and north (region 2) parts of the F-D fault zone including the original and declustered earthquake databases are plotted in Fig. 3. As shown in Figs 3a and 3b, there is not any important fluctuation in seismicity between 1967 and 1975 for both regions. A little change was reported from 1975 to 1983 for region 1 and from 1975 to 1986 for region 2. However, seismic activity progressively increases after 1983 for region 1 and after 1986 for region 2. In addition, there is an important increasing trend in seismicity in two regions after the 1990s, especially from 2010. As seen in Fig. 3, the cumulative number curve of declustered catalogs with larger than or equal to Mc-value as a function of time has a smoother slope than that of original catalogs. Thus, we can clearly interpret that declustering process has removed the dependent events from the original catalogs and this process has supplied more robust, reliable and homogeneous earthquake catalogs.

Time and magnitude histograms for region 1 and region 2 are shown in Figs 4 and 5, respectively. The maximum increases in the earthquake numbers were observed between 1980 and 1985, and there are clear

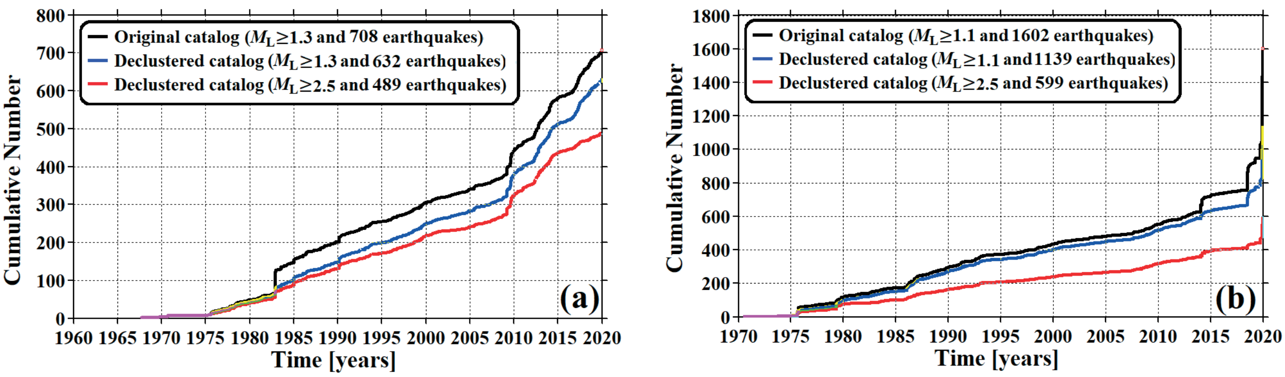

Fig. 3 Cumulative numbers of earthquakes in and around the F-D fault zone with time for the original and declustered catalog for **(a)** the south part (region 1) and **(b)** the north part (region 2)

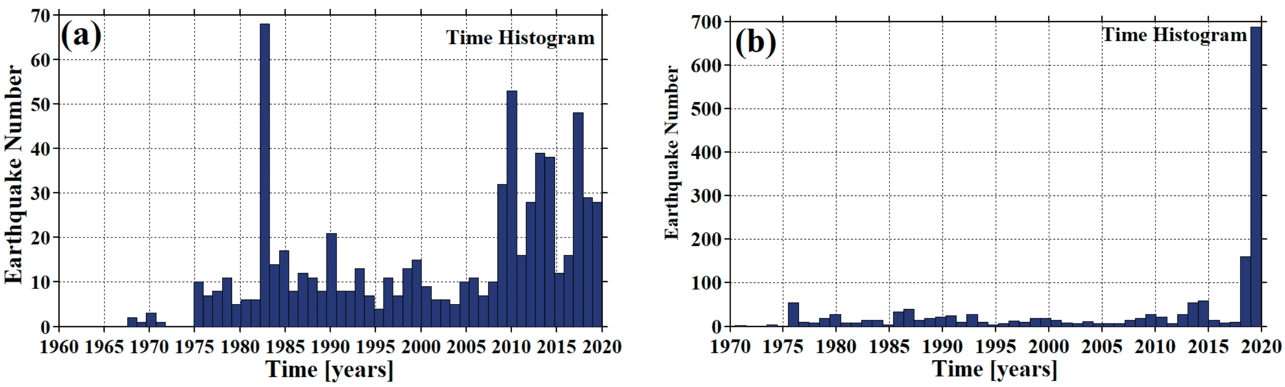

Fig. 4 Time histograms of earthquakes in and around the F-D fault zone for **(a)** the south part (region 1) and **(b)** the north part (region 2)

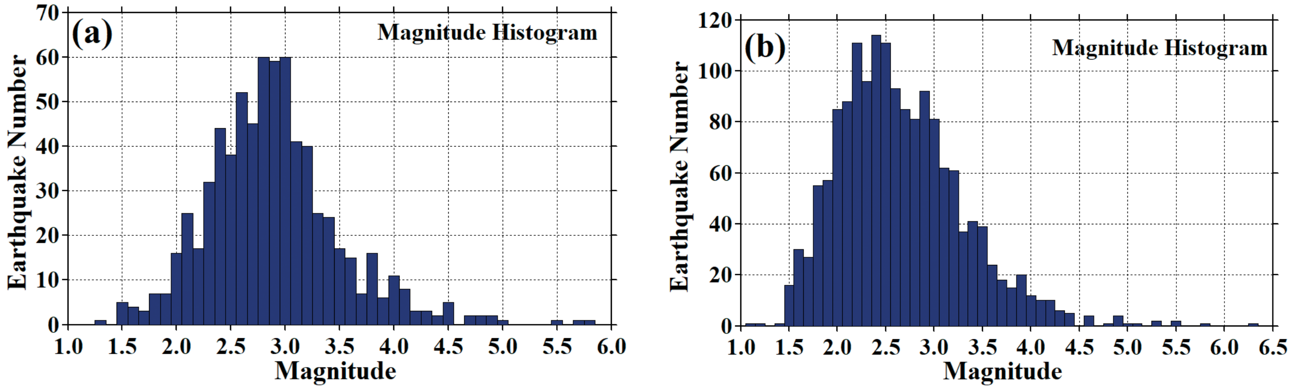

Fig. 5 Magnitude histograms of earthquakes in and around the F-D fault zone for **(a)** the south part (region 1) and **(b)** the north part (region 2)

increases in the number of earthquakes between 2010 and 2020 for region 1 (Fig. 4a). As seen in the time histogram for region 2 (Fig. 4b), there are small increases in the number of earthquakes from 1975 to 2019. However, the maximum increases in the earthquake number can be shown after 2019. Besides the time histograms, magnitude histograms were mapped for two regions of the F-D fault zone. The earthquake magnitudes in these two regions change between 1.1 and 6.3, and the numbers of earthquakes have an exponential decay rate from the smaller to larger sizes. Many of the earthquake magnitudes change from 2.5 to 3.5 levels for region 1 (Fig. 5a), and from 1.5 to 4.0 levels for region 2 (Fig. 5b). Maximum magnitude levels can be seen at $M_L = 2.5$ for both two regions.

As stated in earlier parts, temporal changes in *Mc*-value are highly effective on the estimation of seismic quiescence *Z*-value and seismotectonic *b*-value, as well as the probability and recurrence time. For this reason, the assessments of magnitude completeness with time were realized by a moving window technique with the maximum curvature method supplied by *ZMAP*. *Mc*-values were estimated for samples of 50 events/window for region 1 with the catalog including 708 earthquakes of $M_L \geq 1.3$ (Fig. 6a) and 85 events/window for region 2 with the catalog consisting of 1602 earthquakes of $M_L \geq 1.1$ (Fig. 6b). As seen in Fig. 6a, *Mc*-value changes in and around 3.0 from 1967 to 2013, whereas it has a decreasing trend after 2013 and has a value around 2.5. After 2015, *Mc*-value smaller than 2.5 can be observed for region 1. For region 2, *Mc*-value is relatively high and varies from 2.5 to 3.1 between 1967 and 1985, while it changes around 2.5 after 1990 (Fig. 6b); however, there are some fluctuations between 1.8 and 3.5 from 2018 to 2020. These large values result from a strong earthquake series after 2018. It is well known that time variation of *Mc*-value has generally a non-stable value and this type of analysis must be the first and most important stage since it is a very significant parameter for the *b*-value and *Z*-value statistics. As a remarkable fact, an average of *Mc* = 2.5 for two regions of the F-D fault zone well represents the database.

Magnitude-frequency distributions of the earthquakes for two parts of the F-D fault zone are plotted in Fig. 7. It is well known that the maximum likelihood method gives a more powerful estimation than the least-square method (Aki 1965). Therefore, this method was preferred to estimate the *b*-value of G-R relation. For the south part (region 1), *b*-value was calculated as 0.83 ± 0.06 with *Mc* = 2.5 using all 708 events with $M_L \geq 1.3$ (Fig. 7a). For the north part (region 2), *b*-value was estimated as 0.85 ± 0.06 with *Mc* = 2.5 using all 1602 earthquakes with $M_L \geq 1.1$.

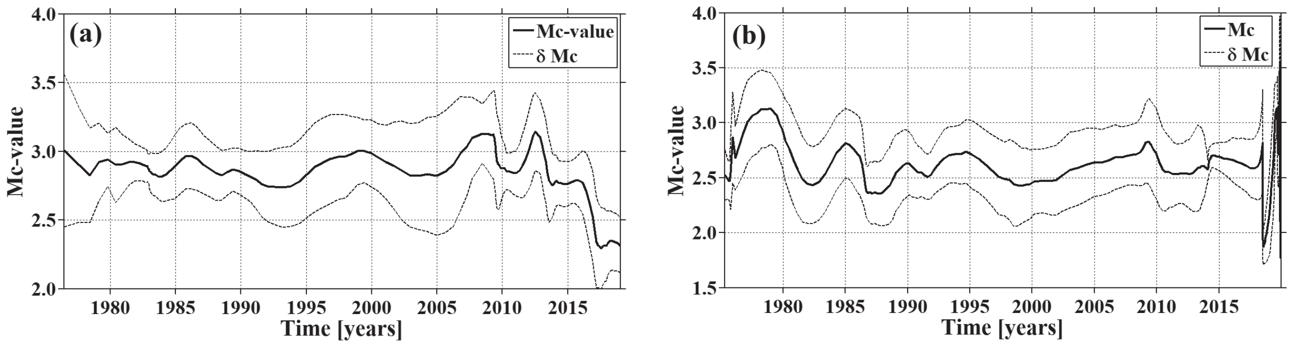

Fig. 6 Magnitude completeness, *Mc*-value, as a function of time in and around the F-D fault zone for **(a)** the south part (region 1) and **(b)** the north part (region 2). Standard deviations, δMc, are also shown

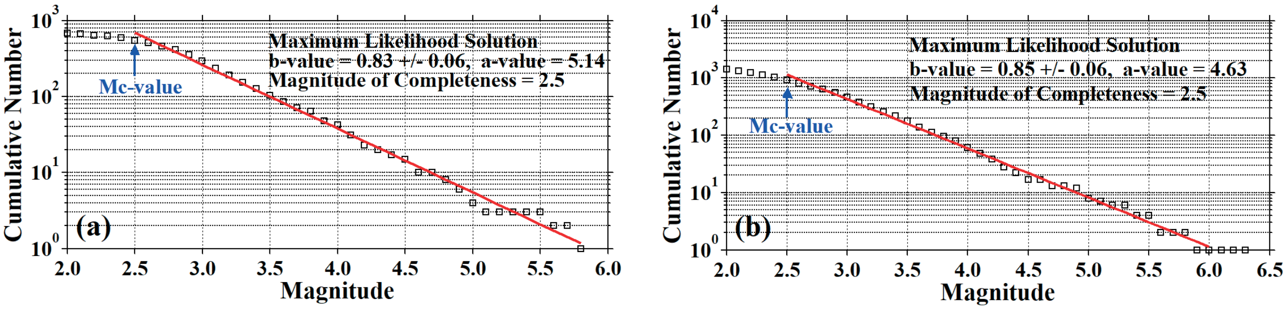

Fig. 7 Gutenberg-Richter relations for **(a)** the south part (region 1) and **(b)** the north part (region 2) of the F-D fault zone. *b*-value, its standard deviation, *Mc*-value and *a*-value are also given

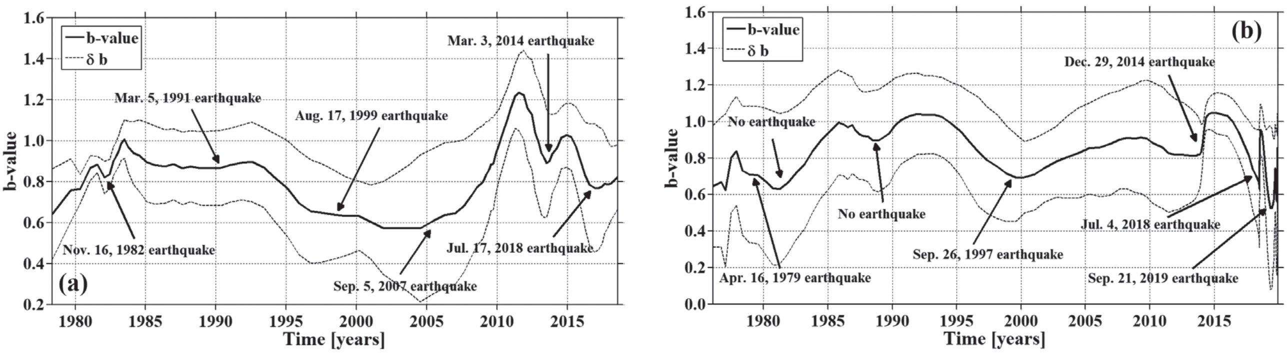

Fig. 8 *b*-value changes as a function of time for **(a)** the south part (region 1) and **(b)** the north part (region 2) of the F-D fault zone. Standard deviation of *b*-value is also given. Arrows show decreases in *b*-value before the occurrences of strong earthquakes

The average *b*-value is suggested as nearly equal to 1.0 (Frohlich, Davis 1993) and tectonic earthquakes are represented with a *b*-value between 0.5 and 1.5. As stated in Frohlich and Davis (1993), a smaller *b*-value may be related to a low heterogeneity degree of medium, higher stress concentration or high strain in the region. A detailed analyses of the *b*-value dependence on the interval size, maximum magnitude, sample size and curve fitting models were provided by different authors mentioned above. Also, the *b*-value is mostly related to the relative number of small and large magnitude earthquakes. A small *b*-value shows a large proportion of large magnitude earthquakes or *b*-values may show slight increases when a larger magnitude levels were not included in the estimations. There are 293 events for region 1 and 458 events for region 2 with magnitude $M_L \geq 3.0$. As seen from the figures, *b*-values for two regions are smaller than the average *b*-value of 1.0 and, consequently, these small *b*-values may indicate an increase of shear stress in the north and south parts of the F-D fault zone in the recent years. Also, these relatively small *b*-values may result from relative abundance of earthquakes having a larger magnitude with $M_L \geq 3.0$. As a remarkable fact, we can say that magnitude-frequency distributions of earthquake catalogs for all regions are well defined with the G-R power law having a characteristic *b*-value close to 1.0.

The *b*-value changes as a function of time for two parts of the F-D fault zone are given in Fig. 8. In the estimation of temporal *b*-value, a sample size of 75 events was used for region 1 and 100 events for region 2. Many systematic decreases in *b*-values were observed before some strong earthquake occurrences in regions 1 and 2. There are decreasing trends in *b*-value smaller than 1.0 before some strong main shocks such as 16 November 1982, 5 March 1991, 17 August 1999, 5 September 2007, 3 March 2014 and 17 July 2018 earthquakes in region 1 (Fig. 8a), whereas some declines in *b*-value are not related to the occurrence of a main shock in region 2. However, clear decreases can be seen from Fig. 8b for region 2 such as 16 April 1979, 26 September 1997, 29 December 2014, 4 July 2018 and 21 September 2019 earthquakes. Temporal changes of *b*-values are one of the most important precursors for earthquake occurrences and many factors can affect these changes. The changes in *b*-value as a function of time show a tendency to decrease before the occurrence of large earthquakes (Öztürk 2011; Prasad, Singh 2015). Öztürk (2011) observed great decreases before the occurrences of several large earthquakes in Turkey such as 17 August 1999 İzmit, 12 November 1999 Düzce, 27 January 2003 Tunceli, and 1 May 2003 Bingöl earthquakes. Prasad and Singh (2015) observed correlation between a small *b*-value for a one-year time interval and the occurrence of large main shocks. They suggested that changes in *b*-value can be used to forecast a major earthquake. We can point out that the decreasing trend in *b*-value before the occurrences

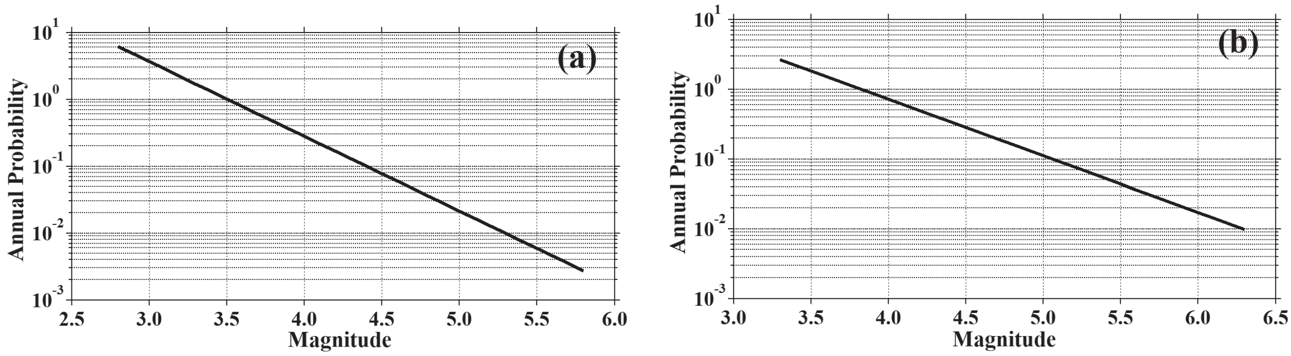

Fig. 9 Annual probabilities for different magnitudes of earthquake occurrences for **(a)** the south part (region 1) and **(b)** the north part (region 2) of the F-D fault zone

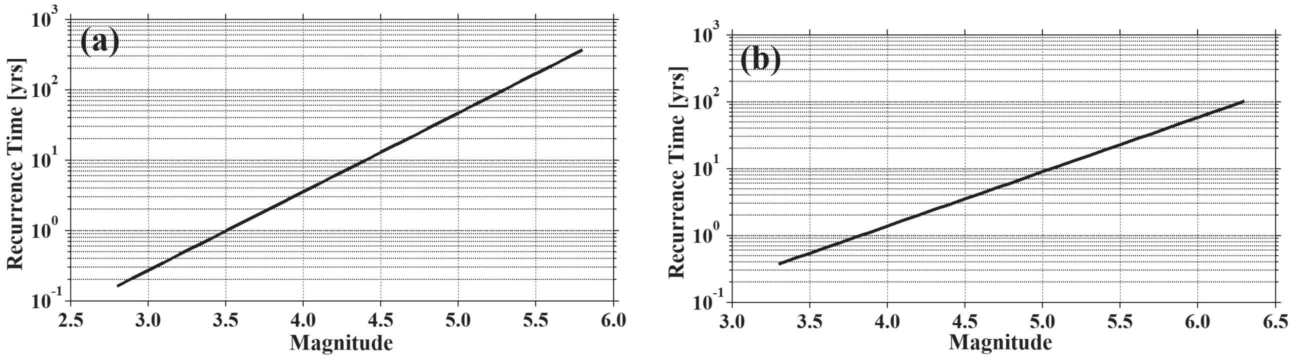

Fig. 10 Recurrence times for different magnitudes of earthquake occurrences for **(a)** the south part (region 1) and **(b)** the north part (region 2) of the F-D fault zone

of some strong main shocks may result from a stress increase. Also, sudden increase in temporal *b*-value may be related to the reduced stress in these times after the main shocks. Thus, these changes are very important for earthquake forecasting, and we can interpret that these fluctuations can be an indicator of the next earthquake in the north and south parts of the F-D fault zone.

For the description of temporal behaviours of earthquakes, estimation of annual probabilities and recurrence times of strong/large earthquake occurrences are very important. Therefore, this comprehensive statistical study includes these types of assessments. The results of annual probabilities and recurrence times for different magnitude sizes in two parts of the F-D fault zone are plotted in Figs 9 and 10, respectively. Annual probabilities of earthquake distributions for the south part (region 1) have the values from 1 to 6 for the magnitude sizes from 2.5 to 3.5, and the values lower than 1 for the magnitude sizes larger than 3.5 (Fig. 9a). However, annual probabilities of the earthquake distributions for the north part (region 1) have the values from 1 to 3 for the magnitude sizes from 3.0 to 3.8, and the values lower than 1 for the magnitude sizes larger than 3.8 (Fig. 9b). Figure 10a shows the recurrence times of different earthquake occurrences for region 1. Relatively smaller recurrence times (<1.0) were estimated for the magnitudes smaller than 3.5, and the time intervals between 1 and 10 years for the earthquake magnitudes from 3.5 to 4.5. In addition, the values between 10 and 50 years can be expected for the magnitude ranges between 4.5 and 5.0, whereas the values greater than 50 years can be considered for the magnitude levels greater than 5.0. The recurrence times of different earthquake occurrences for region 2 are plotted in Fig. 10b. Relatively smaller recurrence times (<1.0) were calculated for the magnitudes smaller than 3.8, and the time intervals between 1 and 10 years for the earthquake magnitudes from 3.8 to 5.0. Also, the values between 10 and 50 years can be expected for the magnitude ranges between 5.0 and 6.0, while the values greater than 50 years can be considered for the magnitude levels larger than 6.0. It is suggested that the earthquake catalog must be declustered and a completeness analysis must be done for the statistical evaluation of earthquake behaviours, especially in the recurrence time analyses of earthquakes (Joseph *et al.* 2011). For this reason, declustered earthquake catalogs were used in these calculations. Results of analyses for the annual probabilities and recurrence times suggest an existing seismic potential in the F-D fault zone in the intermediate/long terms for the possibility of strong/large earthquake occurrence ($M_L \geq 5.0$).

Spatial variations of *b*-value were plotted by using a mowing window technique in *ZMAP* with a sample of 300 earthquakes/window for region 1 and with a sample of 350 earthquakes/window for region 2. These changes were prepared by a spatial grid of 0.01 × 0.01° in latitude and longitude for both two regions. Declustered earthquake catalogs with $M_L \geq 2.5$ including 489 events for region 1 and 599 events for region 2 were used for these analyses. As seen in Fig. 11a, regional distribution of *b*-value changes nearly between 0.7 and 1.1 for region 1. As stated in Frohlich, Davis (1993), the *b*-value of earthquake distributions is well represented by G-R relation with an average value of b = 1.0. Depending on this statement, the areas with the larger *b*-values (>1.0) were observed in the south part of the region 1 including Lushnje, Fieri and Frakull. However, the regions with the lower *b*-values (<0.9) were generally calculated in the north part of the region 1, including Tirana and Durrës. The spatial distribution of *b*-value of region 2 is shown in Fig. 11b. The spatial distribution of *b*-value changes approximately between 0.7 and 1.2 for region 2. The regions with the larger *b*-values (>1.0) were observed in the southeast part of region 2 including Lushnje. However, the regions with the lower *b*-values (<0.9) were generally calculated in all other parts of region 2 including Tirana, Durrës and Lezha. The regions with higher *b*-values have generally a larger proportion of small-magnitude events. However, the regions with smaller *b*-values represent the regions in which great-magnitude events occur more often. In several parts of the F-D fault zone, relatively small *b*-values were computed, and it is accepted that smaller *b*-values make a sign of a higher stress release. Therefore, the smallest *b*-values may be an evidence of a low heterogeneity degree and high strain due to the seismotectonics of the F-D fault zone. These small *b*-values can also be related to the stress to build up over time and to be released by earthquakes that are less frequent but large in magnitude (Öncel, Wilson 2002). As mentioned in many literature studies, low *b*-values may indicate the regions in which the next possible earthquake will occur. Thus, a low *b*-value can be used to forecast future earthquakes in these regions, and therefore, special attention must be given to these areas of the F-D fault zone with small *b*-values.

In order to characterize seismic activity rate changes, spatial variations of standard normal deviate *Z*-value in two parts of the F-D fault zone were mapped at the beginning of 2020 (Fig. 12). For this purpose, each region was divided into regional grids of points with a size of 0.01 × 0.01° in latitude and longitude. The nearest earthquakes, N at each node were considered as 50 earthquakes for both two regions. Earthquakes distribution was binned into many binning spans of 28 days for each grid point, and time window length, T_W, is used as 5.5 years for each region because the quiescence areas are better visible for this time window. In order to map the spatial variations of the standard normal deviate *Z*-value at the beginning of 2020, declustered catalogs with $M_L \geq 2.5$ including 489 events for region 1 and 599 events for region 2 were used. Spatial variations in *Z*-value in the south part of the F-D fault zone (region 1) are displayed in Fig. 12a. As shown in Fig. 12a, there is a region exhibiting precursory quiescence anomalies at the beginning of 2020. This anomaly region was observed among Lushnje-Tirana-Durrës including the middle part of the F-D fault zone. Figure 12b shows the spatial variation of Z-value for region 2. The seismic quiescence region was detected in and around Lezha including the north end of the F-D fault zone.

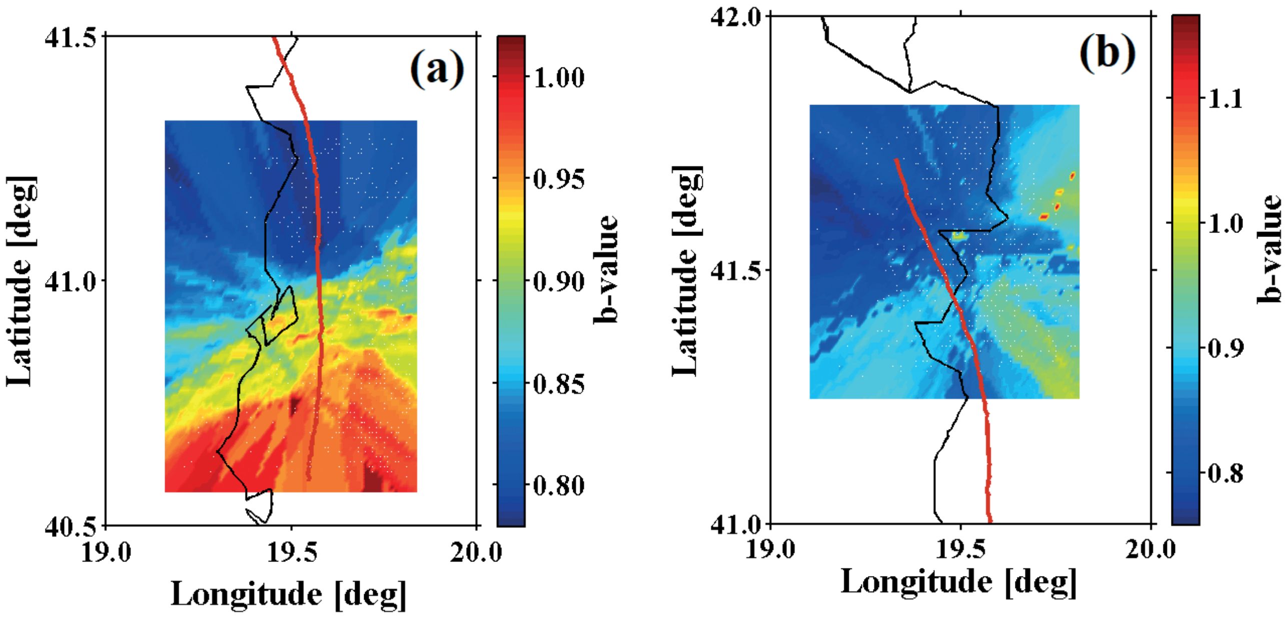

Fig. 11 Spatial variations of *b*-value for **(a)** the south part (region 1) and **(b)** the north part (region 2) of the F-D fault zone. White dots show declustered earthquakes with $M_L \geq 2.5$

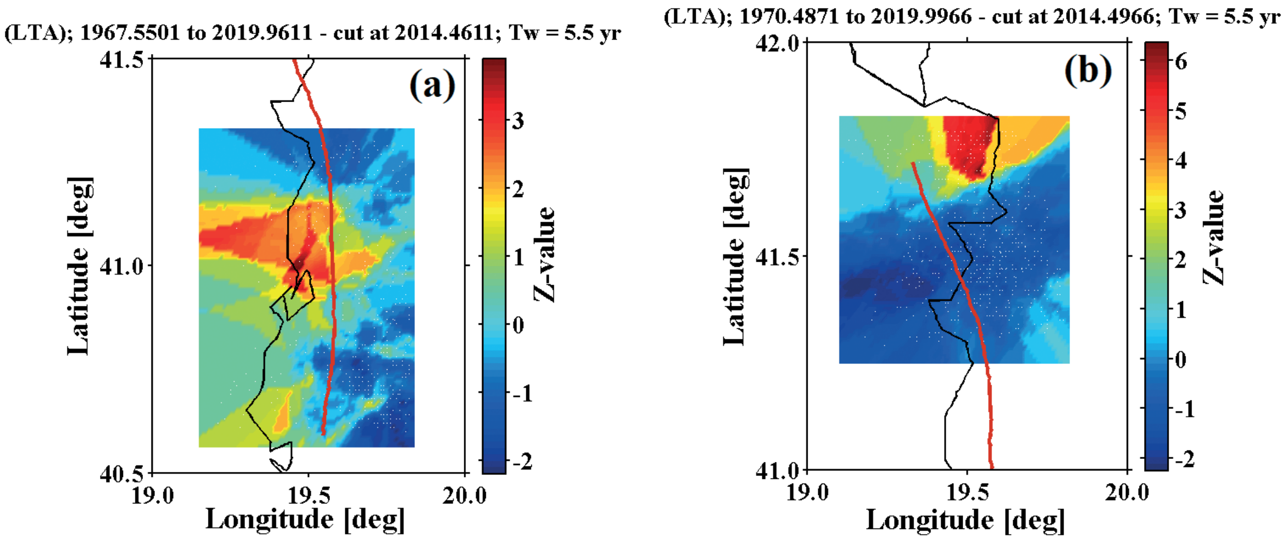

Fig. 12 Spatial changes of *Z*-value at the beginning of 2020 with Tw = 5.5 years for **(a)** the south part (region 1) and **(b)** the north part (region 2) of the F-D fault zone. Declustered earthquakes with $M_L \geq 2.5$ are shown by white dots

For this reason, spatial emphasis should be given to these quiescence regions. Thus, as shown in Figs 11 and 12, a combination of a small *b*-value and a large *Z*-value may provide preliminary and useful keys to evaluate the earthquake potential in and around the F-D fault zone and thus, special emphasis needs to be paid to these anomaly regions.

Spatiotemporal analysis of earthquake activity for different parts of the world have been achieved in many studies, and different statistical models have been used to describe the earthquake characteristics. In recent years, several researchers have used the combination of seismotectonic parameters such as Gutenberg-Richter *b*-value, precursory seismic quiescence *Z*-value, annual probability and recurrence time in order to reveal the possible times and locations of future earthquakes in a given region (e.g. Wiemer, Wyss 1994; Wyss, Martirosyan 1998; Öncel, Wilson 2002; Polat *et al*. 2008; Prasad, Singh 2015; Ali 2016; Rodriguez-Perez, Zuniga 2018; Radziminovich *et al*. 2019; Öztürk 2011, 2013, 2017, 2020; Zuniga *et al*. 2020). The basic idea in these studies is that the regions with a lower *b*-value and a larger *Z*-value may be possible regions for the future earthquake occurrence. For example, a study on the evaluation of earthquake hazard for the western part of Turkey was achieved by Polat *et al*. (2008) by using *b*-value and *Z*-value. They used the maximum likelihood approach to estimate the *b*-value and LTA (*t*) function to map the Z-value. They stated that the areas with a smaller *b*-value or larger Z-value can be interpreted as the most likely region for the future strong earthquake. Öztürk (2011) evaluated the seismic hazard potential for different parts of the North Anatolian Fault Zone, Turkey, using these types of parameters. Some strong earthquakes occurred in this part of Turkey: 22 September 2011 (*M* = 5.6) Refahiye-Erzincan, 30 July 2013 (*M* = 5.3) Gökçeada-Çanakkale, and 3 December 2015 Kığı-Bingöl (*M* = 5.5) earthquakes. Generally speaking, these statistical parameters may be used in the forecasting of the next earthquake locations. Because of a lower *b*-value and the recent quiescence in several regions in and around the F-D fault zone at the beginning of 2020, these anomaly regions are important in the assessment of earthquake potential and hazard.

CONCLUSIONS

In the scope of this study, a comprehensive spatiotemporal evaluation of the recent seismicity in different parts of the Frakull-Durrës fault zone, Albania, was accomplished. For this purpose, the best known and the most frequently used seismotectonic parameters such as *b*-value, *Z*-value, annual probability and recurrence time of earthquake occurrences were preferred. A homogeneous database for local magnitude, M_L was used and it consists of 2310 events with $1.1 \leq M_L \leq 6.3$ between 20 July 1967 and 31 December 2019. For the analysis, the study area was divided into two subregions and Reasenberg's algorithm was used to eliminate the dependent events from the catalog for each region. *Mc*-value was taken as 2.5 for both regions and after these two processes, more robust, reliable and homogeneous earthquake catalogs were obtained to map the regional distributions of *b*-value, *Z*-value and recurrence times. The fundamental conclusions of this statistical study can be given as follows:

(i) *b*-value was calculated as 0.83 ± 0.06 for the south part and 0.85±0.06 for the north part considering *Mc* = 2.5, and there relatively small

b-values may indicate an increase of shear stress in two parts of the F-D fault zone in the recent years. Also, these small b-values can be explained by the relative abundance of earthquakes having larger magnitude.

(ii) Temporal analyses of annual probabilities and recurrence times for specific magnitudes of the south and north parts show that the F-D fault zone has an intermediate/long-term earthquake hazard after 2021 for the possibility of strong/large earthquake occurrences.

(iii) Temporal changes of b-values show significant decreases before the occurrences of a stronger earthquake in south and north parts. These variations can be considered to be related to stress changes in these time intervals and may be preliminary evidences for the future earthquake occurrences in the intermediate/long terms in the F-D fault zone.

(iv) The areas with the smaller b-values (<0.9) were generally observed in the north part of the region 1 including Tirana and Durrës. The areas with the smaller b-values (<0.9) were generally observed in all parts of the region 2 including Tirana, Durrës and Lezha. These regions with small b-values may be related to higher stress release or low heterogeneity degree and high strain due to the seismotectonics of the F-D fault zone.

(v) Several seismic quiescence regions at the beginning of 2020 were observed along Lushnje-Tirana-Durrës including the middle part of the F-D fault zone for region 1 and in and around Lezha including the north end of the F-D fault zone for region 2. Thus, special attention must be paid to these seismic quiescence anomaly regions.

There are many strong/large main shocks in the historical and instrumental periods in the F-D fault zone. Considering the areas having a law b-value and a large Z-value with small recurrence times, one can conclude that these anomaly regions may be interpreted as the possible locations of the future earthquakes. Therefore, the combination of these types of seismotectonic parameters and assessment of the spatiotemporal behaviours together provides significant evidences in the identification of the seismic potential in and around the F-D fault zone. If these behaviours can be described as reliable characteristics of the seismicity, they can contribute to preliminary evaluation of earthquake hazard potential in the Frakull-Durrës fault zone of Albania.

ACKNOWLEDGEMENTS

The authors would like to thank to Dr. Bahruz AHADOV with the other anonymous reviewer for their useful and constructive suggestions in improving this paper. We are grateful to Albanian Seismological Stations, Montenegro Seismological Stations and INGV, MEDNET, and AUTH networks for providing us the earthquake catalog.

REFERENCES

Aki, K. 1965. Maximum likelihood estimate of b in the formula log$N = a – bM$ and its confidence limits. *Bulletin of Earthquake Research Institute Tokyo University 43*, 237–239.

Ali, S.M. 2016. Statistical analysis of seismicity in Egypt and its surroundings. *Arabian Journal of Geosciences 9* (*52*), 2–16.

Aliaj, Sh. 2000. Neotectonics and seismicity of Albania. In: Meco, S., Aliaj, Sh. and Turku, I. (eds.) *Geology of Albania*. Gebruder Borntraeger. Berlin. Stuttgart.

Aliaj, Sh. 2006. The Albanian Orogen: Convergence zone between Eurasia and the Adria Microplate. In: N. Pinter et al. (eds.), *Part of the Nato Science Series*: *IV*: *Earth and Environmental Sciences book series* (NAIV, volume 61), The Adria Microplate: *GPS Geodesy, Tectonics and Hazards* 133–149.

Aliaj, Sh. 2012. *Neotectonics of Albania*. Klan publication. Tirana. [In Albanian].

Aliaj, Sh., Meço, S. 2018. *Neotectonics map of Albania*. At the scale 1:200.000. Albanian Geological Survey, Tirana, Albania.

Aliaj, Sh., Sulstarova, E., Muço, B., Koçiu, S. 2001. *Seismotectonic map of Albania at the scale 1:500.000*. Instituti i Sizmologjisë Tiranë.

Aliaj, Sh., Koçiu, S., Muço, B., Sulstarova, E. 2010. *Seismicity, seismotectonic and seismic hazard assessment in Albania*. Published by Albanian Academy of Sciences.

Arabasz, W.J., Hill, S.J. 1996. Applying Reasenberg's cluster analysis algorithm to regional earthquake catalogs outside California (abstract). *Seismol. Res. Lett. 67* (*2*), 30.

Bega, Z. 1995. The thrust and backthrust systems of External Albanides. D.Sc. Thesis. *Archive of Faculty of Geology and Mining* Tirana. [In Albanian].

Bicoku, T. 1964. Analysis and synthesis of seismic explorations in Periadriatic Depression. D. Sc. Thesis. *Central Archive of Geology* Tirana. [In Albanian].

Frohlich, C., Davis, S. 1993. Teleseismic b-values: Or, much ado about 1.0. *Journal of Geophysical Research 98* (*B1*), 631–644.

Gutenberg, R., Richter, C.F. 1944. Frequency of earthquakes in California. *Bulletin of Seismological Society of America 34*, 185–188.

Joseph, J.D.R., Rao, K.B., Anoop, M.B. 2011. A study on clustered and de-clustered world-wide earthquake data using G-R recurrence law. *Int. J. Earth Sci. Eng. 4*, 178–182.

Kociu, S. 1998. Seismic micro zonation in Preadriatic urban areas of Albania. *Annales Geophysicae* Part IV

Nonlinear Geophysics & Natural Hazard Supplement to volume 16 EGS.
Mazzoli, S., Helman, M. 1994. Neogene patterns of relative plate motion for Africa-Europe: some implications for recent central Mediterranean tectonics. *Geologische Rundschau 83*, 464–468.
Mogi, K. 1962. Magnitude-frequency relation for elastic shocks accompanying fractures of various materials and some related problems in earthquakes. *Bulletin of Earthquake Research Institute Tokyo University 40*, 831–853.
Muço, B. 1994. Focal mechanism solutions for Albanian earthquakes for the years 1964–1988. *Tectonophysics 231*, 311–323.
Muço, B. 2007. Focal mechanism solutions and stress field distribution in Albania. *Albanian Journal of Natural & Technical Sciences 1*, 129–138.
Ormeni, Rr. 2007. The general model of construction of the Albanian earth crust and its seismoactive feature according to the seismological data. PhD thesis, Tirana, Albania.
Ormeni, Rr. 2010. Structure of P, S seismic wave velocities of the Albanian earth lithospheres and its seismoactive features. *Kumi publications* Tirana, Albania.
Ormeni, Rr., Kociaj, S., Fundo, A., Daja, Sh., Doda, V. 2013. Moderate earthquakes in Albania during 2009 and their associated seismogenic zones. *Italian Journal of Geosciences 132* (*2*), 203–212.
Ormeni, Rr., Hoxha, I., Naco, P., Dashamir, G. 2020. The strong earthquake of 26 November 2019 (Mw 6.4) and its associate active tectonic of Durresi region in Albania, *European Geosciences Union*, *General Assembly*, (*EGU2020*), *Abstracts*. Vienna, Austria.
Öncel, A.O., Wilson, T.H. 2002. Space-time correlations of seismotectonic parameters and examples from Japan and Turkey preceding the İzmit earthquake. *Bulletin of the Seismological Society of America 92*, 339–350.
Öztürk, S. 2011. Characteristics of Seismic Activity in the Western, Central and Eastern Parts of the North Anatolian Fault Zone, Turkey: Temporal and Spatial Analysis. *Acta Geophysica 59* (*2*), 209–238.
Öztürk, S. 2013. A statistical assessment of current seismic quiescence along the North Anatolian Fault Zone: Earthquake precursors. *Austrian Journal of Earth Sciences 106* (*2*), 4–17.
Öztürk, S. 2017. Space-time assessing of the earthquake potential in recent years in the eastern Anatolia region of Turkey. *Earth Sciences Research Journal 21* (*2*), 67–75.
Öztürk, S. 2020. A study on the variations of recent seismicity in and around the Central Anatolian region of Turkey. *Physics of the Earth and Planetary Interiors 301* (*106453*).
Polat, O., Gok, E., Yılmaz, D. 2008. Earthquake hazard of the Aegean Extension region (West Turkey). *Turkish Journal of Earth Sciences 17*, 593–614.
Prasad, S., Singh, C. 2015. Evolution of b-values before large earthquakes of $m_b \geq 6.0$ in the Andaman region. *Geologica Acta 13* (*3*), 205–210.
Radziminovich, N.A., Miroshnichenko, A.I., Zuev, F.L. 2019. Magnitude of completeness, b-value, and spatial correlation dimension of earthquakes in the South Baikal Basin, Baikal Rift System. *Tectonophysics 759*, 44–57.
Reasenberg, P.A. 1985. Second-order moment of Central California seismicity, 1969–1982. *Journal of Geophysical Research 90* (*B7*), 5479–5495.
Rodriguez-Perez, Q., Zuniga, F.R. 2018. Imaging b-value depth variations within the Cocos and Rivera plates at the Mexican subduction zone. *Tectonophysics 734–735*, 33–43.
Sulstarova, E. 1986. Focal mechanism of earthquakes and present-day tectonic stress field in Albania. D.Sc. Thesis. Archive of Seismological Institute, Tirana (In Albanian).
Sulstarova, E., Kociaj, S., Aliaj, Sh. 1980. *Seismic regionalization of PSR of Albania*. Publishing House of "*8 Nentori*" Tirana, 1–297.
Utsu, T. 1971. Aftershock and earthquake statistic (III): Analyses of the distribution of earthquakes in magnitude, time and space with special consideration to clustering characteristics of earthquake occurrence (1). *Journal of the Faculty of Science*, *Ser. VII* (*Geophysics*) *3*, 379–441. Hokkaido University.
Wiemer, S. 2001. A software package to analyze seismicity: ZMAP. *Seismological Research Letters 72* (*2*), 373–382.
Wiemer, S., Wyss, M. 1994. Seismic quiescence before the Landers (M = 7.5) and Big Bear (M = 6.5) 1992 earthquakes. *Bulletin of the Seismological Society of America 84* (*3*), 900–916.
Wiemer, S., Wyss, M. 2000. Minimum magnitude of completeness in earthquake catalogs: Examples from Alaska, the Western United States, and Japan. *Bulletin of the Seismological Society of America 90* (*3*), 859–869.
Wyss, M., Martirosyan, A.H. 1998. Seismic quiescence before the M7, 1988, Spitak earthquake, Armenia. *Geophysical Journal International 134* (*2*), 329–340.
Zuniga, F.R., Lacan, P., Rodriguez-Perez, Q., Marquez-Ramirez, V.H. 2020. Temporal and spatial evolution of instrumented seismicity in the Trans-Mexican Volcanic Belt. *Journal of South American Earth Sciences 98*, 102390.